ÉCOLE POLYTECHNIQUE FÉDÉRALE DE LAUSANNE

SWISS PLASMA CENTER

The Flux-Coordinate Independent Approach

Farah Hariri [1]

Contributors:

M. Ottaviani[2], Y. Sarazin[2], P. Hill[3], G. Latu[2], M. Mehrenberger[4], E. Sonnendrücker[5], L. Villard[1]

[1] EPFL, Swiss Plasma Center, 1015 Lausanne, Switzerland
[2] CEA Cadarache, Saint Paul Lez Durance, France
[3] University of York, UK
[4] University of Strasbourg, France
[5] Max-Planck-Intstitut, IPP Garching, Germany

Outline

- Motivation: plasma anisotropy
  Inability to simulate X-point geometry
- The flux coordinate independent (FCI) method to deal with plasma anisotropy and X-point geometry
- Relation to various field-alignment methods
- Applications:
  with the FENICIA finite difference code
  with the GYSELA semi-Lagrangian code
  with BOUT++/GRILLIX/FELTOR
- Conclusions

The computational problem

Global, uniform grid, machine like ITER $a = 2m$, $R = 6m$

- Resolve the ion Larmor radius with four grid points, 1mm grid spacing
- Poloidal plane : $N_R \times N_Z = 4000 \times 4000$ points
- Toroidal direction 36000 points

$$N_{\mathrm{points}} \sim \rho_*^{-3} \sim 6 \times 10^{11}, \textbf{ unaffordable}$$

The computational problem

Global, uniform grid, machine like ITER $a = 2m$, $R = 6m$

- Resolve the ion Larmor radius with four grid points, 1mm grid spacing
- Poloidal plane : $N_R \times N_Z = 4000 \times 4000$ points
- Toroidal direction 36000 points

$$N_{\mathrm{points}} \sim \rho_*^{-3} \sim 6 \times 10^{11}, \textbf{ unaffordable}$$

If one could work with a fixed (ρ_*-independent) number of toroidal points:

- $N_R = N_Z = 4000$, as before
- Perhaps $N_\phi = 64$

$$N_{\mathrm{points}} \sim \rho_*^{-2} \sim 10^9, \textbf{ feasible}$$

Achievable with a flux coordinate independent (FCI) method

Turbulence is anisotropic

Solutions of turbulence models have

$L_{\parallel} \sim qR,\ L_{\perp} \sim \rho_i,$

$$\nabla_{\parallel} \ll \nabla_{\perp}$$

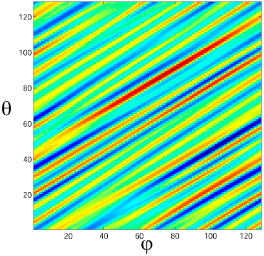

Fluctuations in the (φ,θ) plane

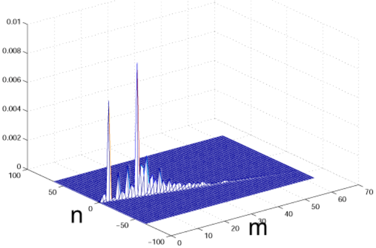

Spectrum in the (n,m) plane

⇨ Substantial waste of computer resources when using a uniform grid spacing

Motivations (1): Anisotropy allows for a reduction of the number of grid points

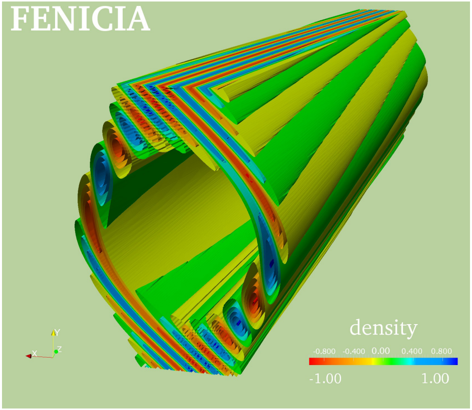

Key considerations:

a) Point reduction can be carried out in almost any direction

b) Information about a function at *missing* grid points can be reconstructed

c) Derivatives can be carried out using the interpolated values at missing grid pts

Motivations (2): Tackling the X-point geometry

X-points in Magnetic Islands & in Tokamak Configurations are **singular**

Neoclassical island in ITER

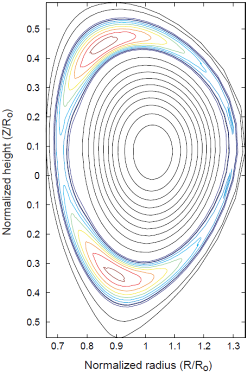

Tokamak configuration

q diverges at the X-point

$\Longrightarrow$ It is numerically challenging to implement $\nabla_{||}$ in the X-point neighborhood

An extreme case: $\nabla_{\parallel} = 0$ on a rational surface

Single helicity solution

$$f(r,\theta,\varphi) = f(r, m\theta - n\varphi)$$

In order to reconstruct the **full** dependence of f on the three coordinates

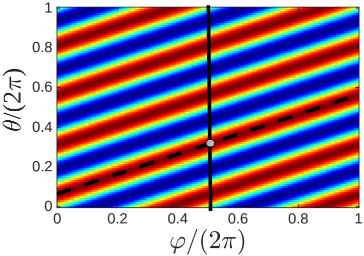

one needs the dependence on r **and**

- the dependence on θ (at any given value of φ), **but not** that on φ, or
- the dependence on φ (at any given value of θ), **but not** that on θ, or
- the dependence on any line on the (θ,φ) plane **not parallel** to the magnetic field

The usual case: $\nabla_{\parallel} \approx 0$

Multiple helicity solutions, weak parallel gradient, on a discretised domain

$$f = f(r, \theta, \varphi), \qquad \nabla_{\parallel} \sim 1/L_{\text{system}}$$

In order to reconstruct **approximately** but adequately the **full** dependence of f on the three coordinates one needs the dependence on r **and**

- the dependence on θ, to a high accuracy **and** that on φ, to a lesser accuracy or
- the dependence on φ, to a high accuracy, **and** that on θ, to a lesser accuracy or
- the dependence on any line on the (θ,φ) plane **not parallel** to the magnetic field, to a high accuracy, and the dependence on any line on the (θ,φ) plane **not perpendicular** to the magnetic field, to a lesser accuracy

Examples of grids with point reduction

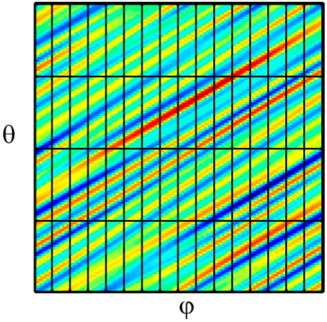

Reduction in θ
Most turbulence codes
Linear ballooning theory

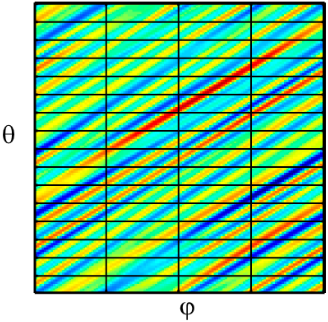

Reduction in φ

2D field-aligning transformations

Ballooning (S. Cowley *et al.*, 1991)

$$\begin{cases} \xi &= \varphi - q(r)\theta \\ s &= \theta \\ \rho &= r \end{cases}$$

$$\nabla_{\parallel} = \frac{1}{q(r)} \frac{\partial}{\partial s}$$

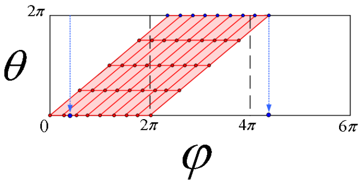

- Reduction of points is in θ
- The small scale dependence is in φ
- Like in the linear ballooning representation
- Most common method in codes
- Can not deal with X-points

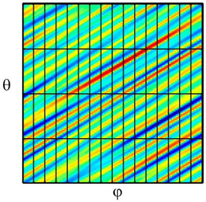

2D field-aligning transformations

with shifts (Scott, 2001)

$$\begin{cases} \xi &= \varphi - q(r)(\theta - \theta_k) \\ s &= (\theta - \theta_k) \\ \rho &= r \end{cases}$$

$$\nabla_\parallel = \frac{1}{q(r)} \frac{\partial}{\partial s}$$

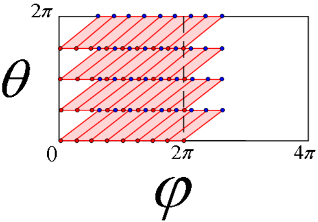

- Reduction of points is in θ
- The small scale dependence is in φ
- Like in the linear ballooning representation
- Most common method in codes
- Can not deal with X-points

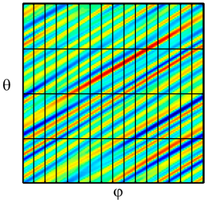

2D field-aligning transformations

Ottaviani, 2009

$$\begin{cases} \xi &= \theta - \frac{1}{q(r)}(\varphi - \varphi_k) \\ s &= (\varphi - \varphi_k) \\ \rho &= r \end{cases}$$

$$\nabla_{\parallel} = \frac{\partial}{\partial s}$$

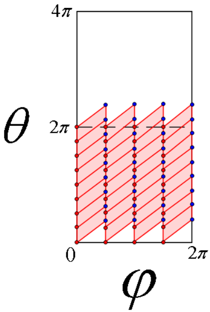

- Reduction of points is in ϕ
- The small scale dependence is in θ
- Not efficient for flexible coding

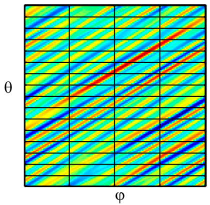

Flux coordinate independent (FCI): point reduction directly in 3D

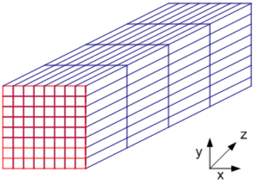

An FCI grid in Cartesian coordinates, with point reduction in z

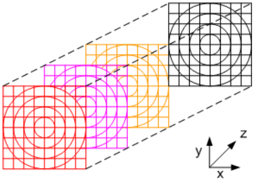

with superimposed circular flux surfaces

F. Hariri and M. Ottaviani, Comp. Phys. Comm. 184, 2419 (2013)

FCI: the grid is independent of the flux surfaces

The same grid can be used for:

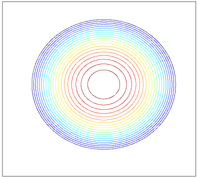

Circular magnetic surfaces

FCI: the grid is independent of the flux surfaces

The same grid can be used for:

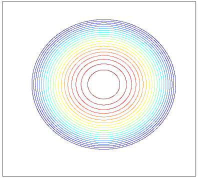

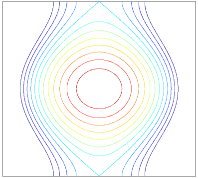

Circular magnetic surfaces and X-point configurations

F. Hariri and M. Ottaviani, Comp. Phys. Comm. 184, 2419 (2013)

Evaluation of differential operators with FCI: finite difference (FD) approach

Parallel derivative:

- Field line equations (straight geometry case)

$$dx/ds = b_x = \partial\psi/\partial y$$
$$dy/ds = b_y = -\partial\psi/\partial x$$
$$dz/ds = 1$$

- Derivative along the line

$$\frac{d}{ds} f(x(s), y(s), z(s)) = -[\psi, f] + \partial f/\partial z = \nabla_{\|} f$$

- 2nd order FD expression

$$\nabla_{\|}^{\mathrm{FD}} f = \frac{f(s+\Delta s) - f(s-\Delta s)}{2\Delta s}$$

The values of f at $s \pm \Delta s$ are obtained by combining **field line tracing** & **interpolation at end points**. $\nabla_{\|}$ can be computed for any magnetic field **including stochastic ones**.

F. Hariri *et al.*, PoP **21**, 082509 (2014)

Parallel derivative with FD and interpolation

The computation of a parallel derivative at a grid point (red point) requires finding the end of a field line arc (blue point)

The value of a function at the blue point is obtained by interpolation in the poloidal plane

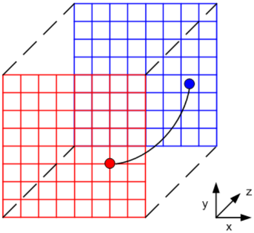

Parallel derivative with FD and interpolation

The computation of a parallel derivative at a grid point (red point) requires finding the end of a field line arc (blue point)

The value of a function at the blue point is obtained by interpolation in the poloidal plane

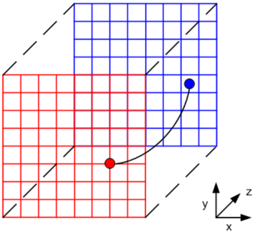

Key points:

- Flux coordinates not needed, only a field line mapper is needed
- The interpolation in the poloidal plane is easily *good* since resolution is *high* to resolve the Larmor radius
- The X-point region *is not special*; no singularity of the field lines, no degeneracy of the coordinate system
- Stochastic field lines do not pose a problem
- Perpendicular (poloidal plane) operations are straightforward

Parallel derivative with FD and interpolation

The computation of a parallel derivative at a grid point (red point) requires finding the end of a field line arc (blue point)

The value of a function at the blue point is obtained by interpolation in the poloidal plane

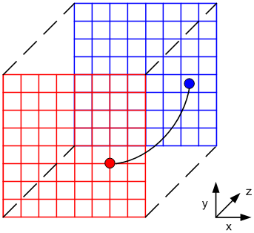

Advantages:

- Reduce the number of points along z
- Can use any coordinate system in the poloidal plane
- Can tackle any magnetic configuration: **X-points**

Likewise, in the toroidal case

- Field line equations:

$$
\begin{aligned}
dR/ds &= R\, B_R/B_\varphi \\
dZ/ds &= R\, B_Z/B_\varphi \\
d\varphi/ds &= 1
\end{aligned}
$$

- Derivative along the field line is:

$$
\frac{d}{ds} f(R(s), Z(s), \varphi(s)) = \frac{RB}{B_\varphi} \nabla_\| f
$$

- Straightforward implementation of FCI by choosing the toroidal angle as a parameter to track the position along a field line

F. Hariri *et al.*, PoP **21**, 082509 (2014)

FCI for kinetic semi-Lagrangian codes

Example: simple electrostatic problem, large scale limit

$$\frac{\partial f_{GC}}{\partial t} + \mathbf{v}_E \cdot \nabla_\perp f_{GC} + v_\parallel \nabla_\parallel f_{GC} + \frac{q}{m} E_\parallel \frac{\partial f_{GC}}{\partial v_\parallel} = 0$$

Equations of motion:

1. Splitting (r, θ) and φ motions
   $\Longrightarrow$ **coupling $\perp$ and $\parallel$ dynamics:**

$$\begin{cases} dr/dt = & v_E.\nabla r \\ d\theta/dt = & v_E.\nabla\theta + v_\parallel / q\,R \end{cases}$$

$$d\varphi/dt = v_\parallel / R$$

2. Splitting v_E and $v_\parallel$ motions using the FCI spirit
   $\Longrightarrow$ **decoupling $\perp$ and $\parallel$ dynamics:**

$$\begin{cases} dr/dt = v_E.\nabla r \\ d\theta/dt = v_E.\nabla\theta \end{cases} \quad \text{and} \quad \begin{cases} d\theta/dt = v_\parallel / q\,R \\ d\varphi/dt = v_\parallel / R \end{cases}$$

Interpolation scheme for $\nabla_{\|}$

- Finding the foot of the trajectories using semi-Lagrangian (backward) method

$$\theta^* = \theta(t) = \theta_i(t+\Delta t) - (v_{\|}/q\,R)\,\Delta t$$
$$\varphi^* = \varphi(t) = \varphi_j(t+\Delta t) - (v_{\|}/R)\,\Delta t$$

- Interpolating to find the distribution function at (θ^*, φ^*)

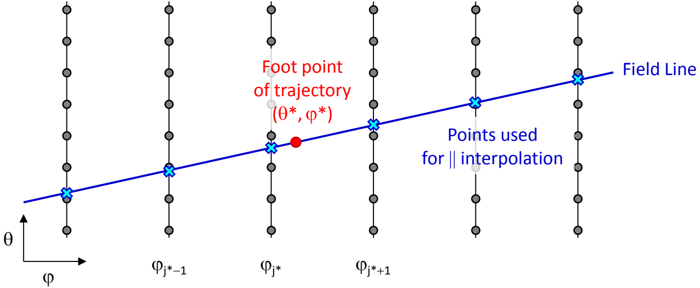

Codes adopting the FCI approach

Part of 3 ER Projects (2015-2017). It is now implemented in:

1. **FENICIA** 3D fluid code
   [F. Hariri and M. Ottaviani, CPC, 2013]
2. **BOUT++** 3D fluid code (York)
   [B. Shanahan, B. Dudson, J. Phys conf. series, 2015]
3. **GRILLIX** 3D fluid (Garching)
   ⟶ A. Stegmeir, talk on Thursday
4. **FELTOR** 3D gyrofluid code (Innsbruck)
   ⟶ M. Held, Poster today
5. **GYSELA** 5D full-f gyrokinetic code (CEA)
   [G. Latu and M. Mehrenberger]

presented by Farah Hariri

Solves a gyrofluid model in cylindrical geometry:

$$\begin{cases} \partial_t \tilde{n} + [\phi, log(n0)] - [\phi, \rho_*^2 \nabla^2 \phi] + C_\parallel \nabla_\parallel u_\parallel = D_n \nabla_\perp^2 \tilde{n} \\ \partial_t u_\parallel + [\phi, u] + C_\parallel (\frac{1}{\tau} \nabla_\parallel \tilde{n} + \nabla_\parallel \phi + \nabla_\parallel T_\parallel) = D_u \nabla_\perp^2 u_\parallel \\ \partial_t T_\parallel + [\phi, T_\parallel] + \frac{2}{\tau} C_\parallel \nabla_\parallel u_\parallel - \chi_{\parallel\parallel} \nabla_\parallel^2 T_\parallel = D_{T_\parallel} \nabla_\perp^2 T_\parallel \\ \partial_t T_\perp + [\phi, T_\perp] - \chi_{\parallel\perp} \nabla_\parallel^2 T_\perp = D_{T_\perp} \nabla_\perp^2 T_\perp \\ \phi = \tilde{n} \end{cases}$$

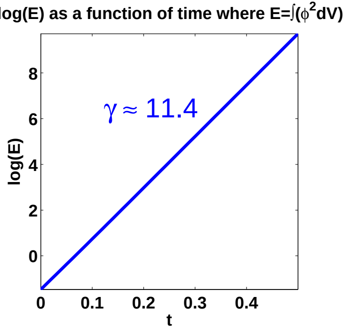

$\gamma_{theory} \approx 11.7$

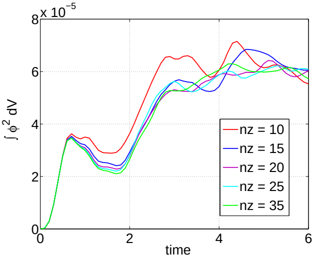

Potential fluctuations level
Convergence at $N_z = 15$

movie: 3D evolution of density fluctuations

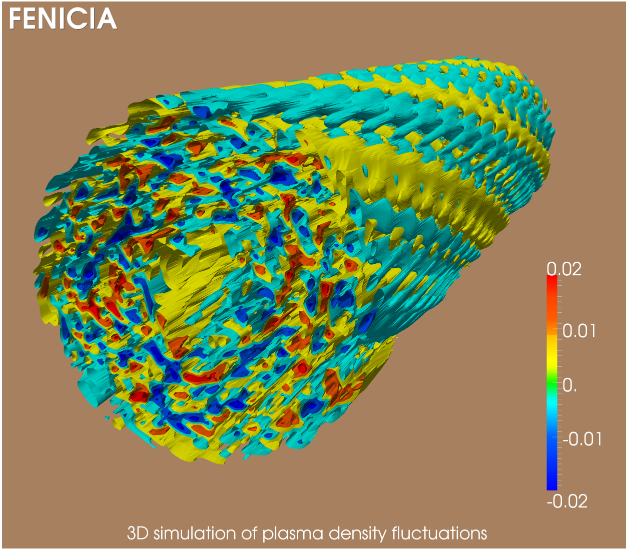

FENICIA: Sound-wave propagation in X-point geometry

Consider an equilibrium with a magnetic island:

$$\psi = -\frac{(x-1)^2}{2} + A\cos(y)$$

in a slab domain periodic in y and z

$$\mathbf{b} \equiv = \nabla \times (\psi\,\mathbf{e}_z) + \mathbf{e}_z$$

$$\nabla_{\|} \equiv b \cdot \nabla = -[\psi, .] + \partial_z$$

Sound wave model

$$\begin{cases} \partial_t \phi + C_{\|}\,\nabla_{\|} u = 0 \\ \partial_t u + \frac{(1+\tau)}{\tau}\,C_{\|}\,\nabla_{\|}\phi = 0 \end{cases}$$

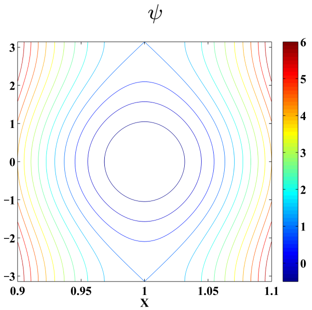

Convergence achieved with analytic solutions at the exterior of the island

Analytic solution of the sound wave model:

$$\begin{pmatrix} \phi(\rho,\eta,t) \\ u(\rho,\eta,t) \end{pmatrix} = \begin{pmatrix} \phi_0(\rho) \\ u_0(\rho) \end{pmatrix} \cos\left[m\,\eta - n\,z - \omega(\rho)\,t\right]$$

with (ρ,η) island flux coordinates and ω the mode frequency

Initial condition

For $(\mathbf{m},\mathbf{n}) = (\mathbf{24},\mathbf{1})$

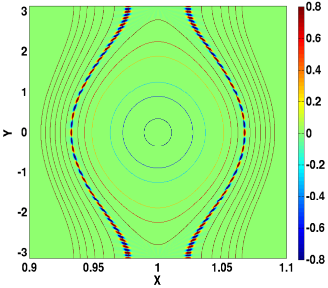

Convergence of num. sol.

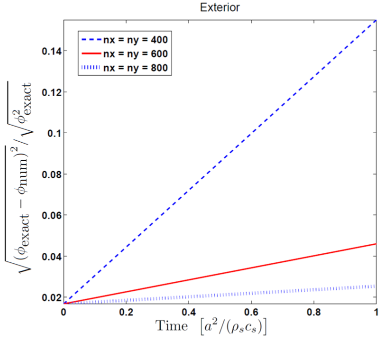

movie: evolution of a perturbation across the separatrix

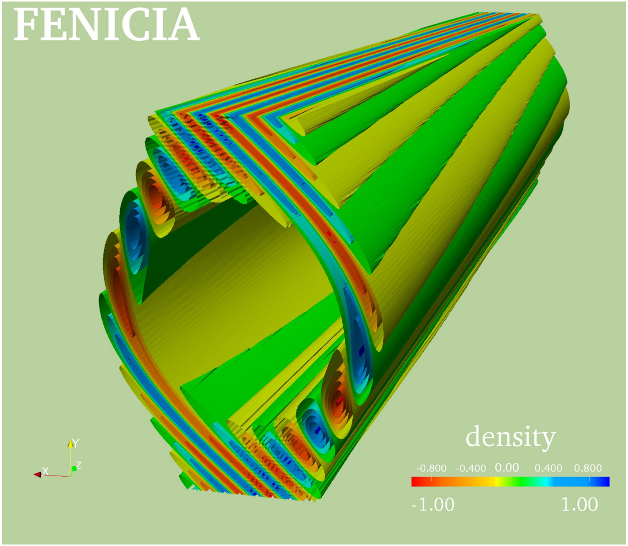

Convergence achieved across the separatrix

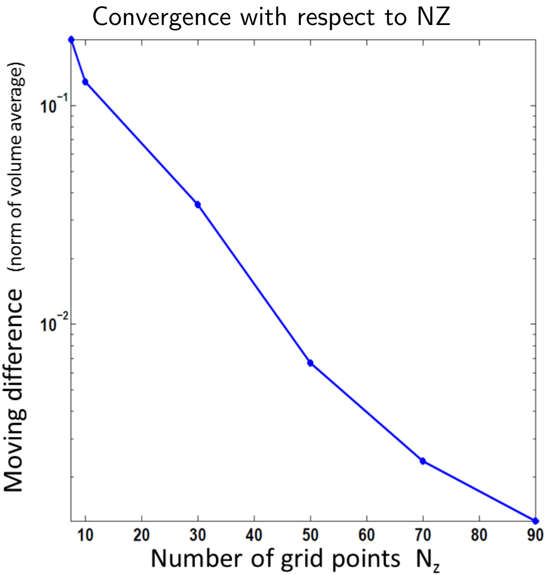

FENICIA main application: Interaction of turbulence with a magnetic island

<u>**Goal:**</u> explore the temperature profile flattening mechanism caused by an island in a turbulent environment. Of interest for the NTM threshold problem.

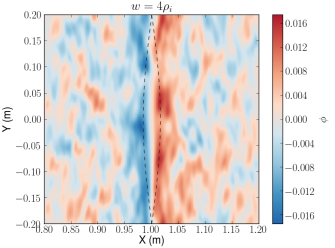

Figure: island width $\omega = 4\rho_i$

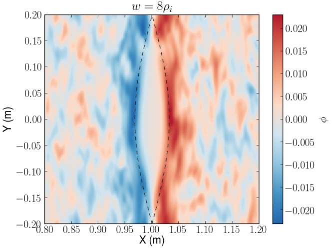

Figure: island width $\omega = 8\rho_i$

Main finding from the island width scan:

Turbulence can cross the separatrix and penetrate $\sim 4\rho_i$ into the island (roughly the turbulence correlation length)

F. Hariri *et al.*, PPCF **57**, 054001 (2015)

GRILLIX: application of FCI in toroidal X-point geometry

presented by Farah Hariri

GRILLIX (A. Stegmeir, see talk on Thursday)

- FCI applied to toroidal X-point geometry
- Discretisation of parallel diffusion
- Based on integral representation for parallel gradient to cope with map distortion
- Hasegawa-Wakatani simulations

Simulation of temperature blob in realistic toroidal geometry (parallel diffusion):

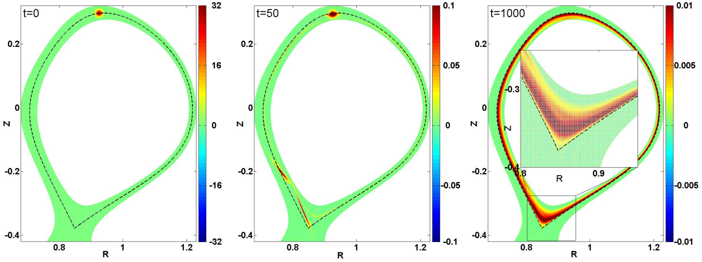

FELTOR: application of FCI in toroidal X-point geometry

FELTOR (M. Held, see Poster today)

- FCI in toroidal X-point geometry run on GPUs
- with discontinuous Galerkin methods
- 3D full-f Gyrofluid model with FLR effects

DW turbulence and ballooning blowout recovered:

Drift-Wave Turbulence In Global X-Point Geometry

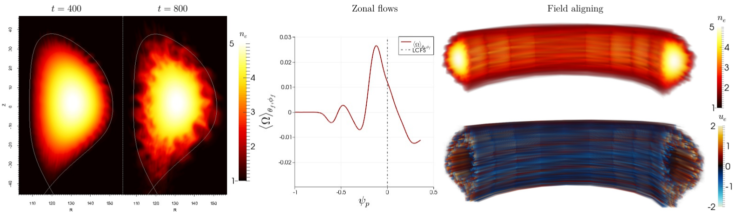

On the left the electron density during an ideal balooning mode blowout is shown. The developed drift-wave turbulent state is given in the center, while on the right the footprint of zonal flows appears for the flux surface averaged vorticity. In the 3D fields of the electron parallel velocity (left) and the electron density (right) the characteristic flute mode structure appears. The spatial resolution is $P_{RZ} = 3$, $P_\varphi = 1$, $N_R = 120$, $N_Z = 160$, $N_\varphi = 20$.

GYSELA code:

Test of ITG growth rate in a 4D ($\mu = 0$) gyrokinetic model.
Comparison: Uniform grid vs FCI semi-Lagrangian method

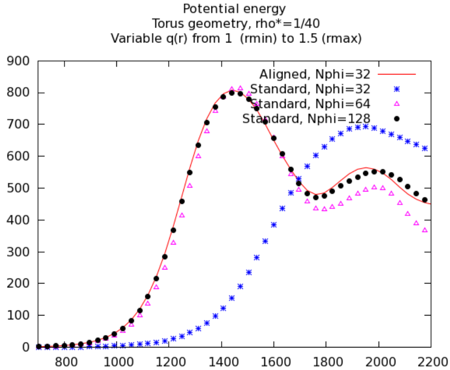

Figure: Potential energy as a function of time

G. Latu *et al.*, https://hal.inria.fr/hal-01098373

Robustness of FCI in semi-Lagrangian schemes

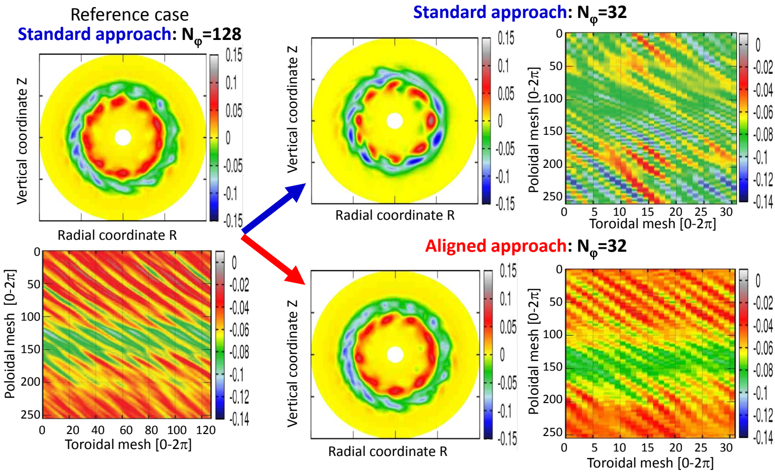

G. Latu *et al.*, 2015 (in preparation)

Summary

- A flux coordinate independent (FCI) method has been devised to exploit the anisotropic nature of plasma turbulent fluctuation and reduce computational needs.

Summary

- A flux coordinate independent (FCI) method has been devised to exploit the anisotropic nature of plasma turbulent fluctuation and reduce computational needs.
- Benefits of the method are:
  - grid independence of magnetic geometry
  - natural applicability to X-point configurations, 3D geometries and stochastic field lines

Summary

- A flux coordinate independent (FCI) method has been devised to exploit the anisotropic nature of plasma turbulent fluctuation and reduce computational needs.
- Benefits of the method are:
  - grid independence of magnetic geometry
  - natural applicability to X-point configurations, 3D geometries and stochastic field lines
- Tests and applications carried out to a variety of situations:
  - drift wave propagation and ITG turbulence in cylindrical geometry
  - sound wave propagation in X-point geometry and application to the problem of turbulence with a magnetic island
  - development and tests of the method for semi-Lagrangian kinetic codes.